The International Archives of the Photogrammetry, Remote Sensing and Spatial Information Sciences, Volume XLVI-3/W1-2022
7th Intl. Conference on Ubiquitous Positioning, Indoor Navigation and Location-Based Services (UPINLBS 2022), 18–19 March 2022, Wuhan, China

AN ADAPTIVE SMARTPHONE HYBRID INDOOR POSITIONING SOLUTION INCORPORATING HETEROGENEOUS SENSORS

Sheng Yang[1], Jingbin Liu[1 *], Xiaodong Gong[1], Gege Huang[1], Fei Yin[1]

[1] State Key Laboratory of Information Engineering in Surveying, Mapping and Remote Sensing, Wuhan University, Wuhan, China – (shengy, jingbin.liu, gongxiaodong, geehuang, whu_yf) @whu.edu.cn

Commission IV, WG IV/5

KEY WORDS: Indoor Positioning, Smartphone Navigation, Pedestrian Localization, Multi-sensor Integration

ABSTRACT:

Indoor positioning algorithms based on Wi-Fi or Bluetooth low energy (BLE) have been widely used for indoor navigation and Internet of Things (IoT) applications, due to their low cost. However, their positioning accuracy is between 2-5 meters, which is insufficient for many emerging applications requiring higher accuracy. New high-precision positioning technologies, such as light, acoustic, and Bluetooth Angle of Arrival (AoA)-based positioning systems, have been developed, and they can achieve decimeter-level positioning accuracy. However, these high-precision positioning technologies suffer from high costs. In this paper, an adaptive smartphone hybrid indoor positioning solution incorporating heterogeneous sensors is proposed to achieve high accuracy and reliable localization. Multiple indoor scenes are identified and the quality of pedestrian movement is detected, thus enabling the adaptive estimation and adjustment of measurement noise and process noise in the filtering procedure. High-precision sensors (i.e. Bluetooth array, acoustic sensors and light sensors) are utilized in the proposed solution as controlling anchors to improve the positioning accuracy. Low-cost sensors (i.e. Wi-Fi, BLE and inertial measurement unit (IMU) sensors), are integrated to achieve wide-area coverage. An autonomous outlier detection method is developed to improve the positioning accuracy and reliability. Experimental results show that the proposed solution can achieve accuracy of 0.98 m in the test scenario.

1. INTRODUCTION

As one of the core technologies of artificial intelligence, indoor positioning will greatly improve people's lives and bring significant commercial value (Davidson, 2017), (Li, 2021), (Harle, 2013). Since the various sensors inherited from smartphones, smartphone-based indoor positioning and navigation is ubiquitous and makes high commercial sense. Currently, Wi-Fi or Bluetooth low energy (BLE)-based methods are successfully applied to the masses. Due to the complexity of indoor environment and the fluctuation of wireless signals, they can typically only achieve a positioning accuracy of 2 to 5 meters. High-precision indoor positioning better than 1 meter is becoming an urgent need.

New high-precision technologies, such as light (Xie, 2018), acoustic (Cao, 2020) and Bluetooth AoA approaches (QUUPPA, 2021), continue to emerge. They can achieve decimeter-level positioning accuracy, but have high application costs. Other high-precision positioning technologies, such as pseudo-satellite (Huggins, 2009), ultra-wideband (Brovko, 2021) and 5G (Huo, 2018), are gradually appearing in the market for indoor positioning. They can achieve centimeter to decimeter positioning accuracy in indoor environments. However, for the application of these high-precision positioning technologies, the facilities and equipment costs are correspondingly high, which will limit their wide application.

Although there are many indoor positioning methods, there is no yet a technology that can effectively solve the indoor positioning problem considering the cost and reliability factors. Multi-sensor intelligent integration and positioning is the future trend of indoor positioning development (Yang, 2021). However, due to the complexity of indoor environments and the diversity of sensors built into smartphones, it remains a challenge to accommodate different sensor noises and different test scenarios in an integrated algorithm. Therefore, in this paper, we propose an adaptive hybrid indoor positioning solution for smartphones, which integrates different types of positioning sensors in off-the-shelf smartphones, to achieve robust and reliable indoor localization.

The main contributions are summarized as follows.

(1) An adaptive integration system based on multi-scene recognition and movement quality monitoring is proposed to realize adaptive estimation of measurement noise and adaptive adjustment of process noise in the filtering procedure. Outlier errors are detected and eliminated online to improve the accuracy and reliability of the integration system.

(2) The proposed hybrid indoor positioning solution exploits a limited number of high-precision positioning sensors as controlling anchors to enhance the accuracy of the hybrid solution, and utilizes low-precision but low- cost positioning sensors to cover a wide area. As a result, the hybrid solution is able to achieve the accuracy of 1 meter in a real location-based services space (e.g. an office building)

(3) By exploiting the high-precision positioning sensors, the hybrid solution adaptively estimates gyro heading drift and personalized parameters of step length model in real time to enhance consistency for different pedestrian users. At the same time, the accuracy of the whole integration system is greatly improved.

In order to verify the reliability of the described method, the proposed multi-sensor integration algorithm was validated in an office building. It utilizes the high-precision sensors as controlling anchors to improve the accuracy of the positioning system, and apply low-cost sensors to achieve the whole-floor localization. At the same time, the high-precision sensors allow correction of gyro heading drift and pedestrian step model errors in multi-sensor integration. Experimental results show

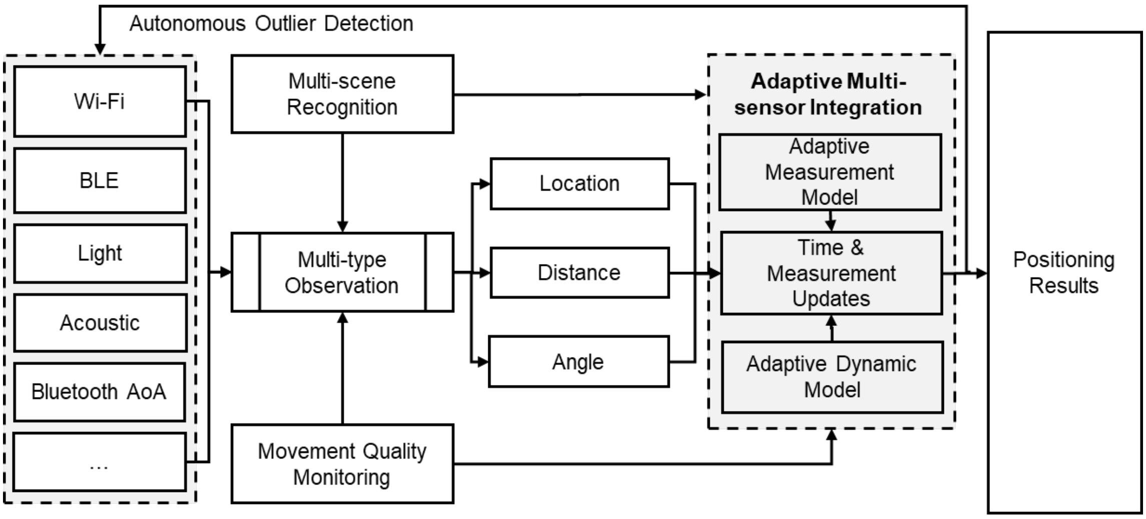

Figure 1. Flowchart of the adaptive multi-sensor integration solution.

that the proposed method combined with heterogeneity sensors achieves better than 1 m positioning accuracy in test scenarios. The remainder of this paper is organized as follows. Section III describes the framework of the adaptive smartphone hybrid indoor positioning solution. Experiments are performed in Section IV. Finally, conclusions are summarized in Section V.

2. FRAMEWORK OF THE ADAPTIVE HYBRID INDOOR POSITIONING SOLUTION

With the development of science and technology, many indoor positioning technologies have emerged and used in practical applications. Due to the complexity of the indoor environment, there is no single method that can effectively solve all indoor positioning problems. Therefore, we propose an adaptive smartphone hybrid indoor positioning solution, which integrates various types of sensors, to achieve robust and reliable indoor positioning. It takes advantage of the complementary nature of different localization methods and considers how to adaptively integrate different sensor information. The detailed flowchart of the adaptive multi-sensor integration solution is shown in Fig. 1. In this positioning system, unscented Kalman filter (UKF) is used in the integration system to solve the pedestrian movement nonlinearity problem. Multi-type observation calibration is introduced into the positioning system to accommodate multiple types of measurement information. It integrates three types of observation data, including location, distance and angle. In order to implement an adaptive integration system, different indoor scenes are identified and pedestrian movement quality is reliably monitored. And the outliers of various measurements are detected and eliminated by the integration solution. Finally, a stable and adaptive multi-sensor integration solution is achieved.

2.1 UKF-based Integration Algorithm

The UKF is utilized to incorporate measurements of different sensors, as it is adapted to the estimation of nonlinear problems. It uses a deterministic sampling approach to accurately capture the posterior mean and covariance up to third order (Taylor series expansion) (Julier, 2004). For this UKF-based integration system, the state vector is designed as follows:

$$x = \begin{bmatrix} e & n & v & \theta & s & b \end{bmatrix}^T \tag{1}$$

where e and n are local coordinates in the east and north direction, respectively. v denotes the pedestrian speed and s denotes the scale factor of step length model to describe the heterogeneity of pedestrian steps. θ and b denote the pedestrian heading angle and the bias of the heading angular velocity, respectively.
The time update equation can be expressed as follow:

$$\begin{aligned} e_k^- &= e_{k-1}^+ + v_k^- \cdot \Delta t \cdot \sin\theta_k^- + w_1 \\ n_k^- &= n_{k-1}^+ + v_k^- \cdot \Delta t \cdot \cos\theta_k^- + w_2 \\ v_k^- &= v_{k-1}^+ + s_k^- \cdot \Delta v + w_3 \\ \theta_k^- &= \theta_{k-1}^+ + \Delta\theta - b_k^- \cdot \Delta t + w_4 \\ s_k^- &= s_{k-1}^+ + w_5 \\ b_k^- &= b_{k-1}^+ + w_6 \end{aligned} \tag{2}$$

where the subscript k denotes the epoch, the superscript - and + are the prediction and update of the state vector, respectively. Δv and $\Delta\theta$ are the increment of pedestrian's speed and heading angle from the PDR algorithm (Yang, 2021). Δt is the time interval and $w_{i=1,2,\ldots,6}$ is the process noise.
The measurement update equation is as follows:

$$z_k = h(x_k^-) + l \tag{3}$$

where z_k is the measurement vector, $h()$ is the nonlinear function between the state vector and the measurement vector, and l is the measurement noise.
The detailed solution process of UKF can be found in (Julier, 2004). It is worth to mention that the initial velocity of the system is given by the PDR and the initial heading is obtained by the magnetometer. The errors in velocity and heading will converge after the integrated solution is stabilized.

2.2 Multi-type Observation Models

There are many different positioning methods for smartphone indoor positioning. The main types of positioning observations from different sensors include location, distance and angle. In details, Wi-Fi or Bluetooth fingerprinting methods provide location type observations, while the Bluetooth AoA system provides angle type observations. Audio-based localization techniques or radio-frequency signal ranging methods provide distance type observations. light-based methods can provide both distance and angle observations. They are sent into the UKF fusion solution for measurement updates.

$$\begin{aligned} z_P &= \binom{e_P}{n_P} = \binom{e_k^-}{n_k^-} + l_1 \\ d_D &= \sqrt{(e_k^- - e_D)^2 + (n_k^- - n_D)^2} + l_2 \\ \theta_A &= \arctan\frac{e_k^- - e_A}{n_k^- - n_A} + l_3 \end{aligned} \quad (4)$$

where z_P represents the position measurement vector, d_D represents the distance measurement vector, θ_A represents the azimuth measurement vector. $l_{i=1,2,3}$ represents the corresponding measurement noises.

The integration solution is achieved by fusing different sensors based on the UKF tight combination method. It is flexible for different types of observations and can be switched quickly in real-time positioning.

2.3 Multi-scene Recognition

There are many scenes in the indoor environment, which can usually be divided into three categories, i.e., wide area scenes (e.g., halls, lobbies and plants), office scenes and corridor scenes. Due to the diversity of indoor environments, each positioning signal, especially radio-frequency signal, is often subject to non-line of sight or multi-path interference. This leads to variability in the performance of the same positioning signal in different indoor scenes. In order to overcome the effect of indoor scene changes on localization, a multi-scene recognition approach is proposed in this section. This method combines the coarse position provided by Wi-Fi/BLE fingerprinting method and the pedestrian walking straight-line distance from PDR (Yang, 2021) to distinguish different indoor scenes in complex indoor environments.

Specifically, when a pedestrian walks freely in an indoor environment, his or her fingerprinting result from Wi-Fi/BLE are automatically recorded. If several successive recorded fingerprinting results belong to the same scene, then the corresponding pedestrian is likely to be in that scene. In addition, the trajectory of pedestrians walking indoors is also related to the indoor scene. In room areas, pedestrians often need to walk a fixed track due to the public items in the room. In the corridor area, pedestrians need to walk a long straight track. Combining the straight-line distance traveled by pedestrians and the successive recorded fingerprinting results, the estimated scene id calculated as follows:

$$\text{The estimated scene} = \begin{cases} \text{wide scene}, P_M \in \text{wide scenes and } (D \ge d_1 \,\|\, T \ge t_1) \\ \text{office scene}, P_M \in \text{office scenes and } (D \ge d_2 \,\|\, T \ge t_2) \\ \text{corrider scene}, P_M \in \text{corrider scenes and } (D \ge d_3 \,\|\, T \ge t_3) \end{cases} \quad (5)$$

where P_M means M continuously recorded fingerprinting location, D is the straight-line distance traveled by pedestrians from PDR algorithm, T is the stationary time of pedestrians. $d_{i=1,2,3}$ is the straight-line distance threshold and $t_{i=1,2,3}$ is the stationary time threshold. These thresholds depend on the building map information.

When several consecutive fingerprinting locations belong to the same scene and the pedestrian walks a certain straight line distance or is stationary for a period of time, the corresponding scene will be automatically recognized.

2.4 Movement Quality Monitoring

Smartphone-based multi-sensor integration systems mostly rely on PDR for location recursion. In practice, however, PDR is often affected by pedestrian movement. PDR step detection is prone to mis-judgment when pedestrians raise their arms up and down or switch smartphone postures while walking. The heading offset between the smartphone's heading and the user's direction of movement is susceptible to change when the pedestrian moves randomly. In order to improve the robustness of the PDR-based integration system, a movement quality monitoring method is proposed in this section. It mainly detects the continuity indicator of pedestrian walking and the dynamic indicator of the smartphone through the built-in sensors of the smartphone.

Based on the smartphone horizontal angle change, we present a dynamic indicator $A_{indicator}$ for pedestrian motion:

$$A_{indicator} = \sqrt{\omega_e^2 + \omega_n^2} \quad (6)$$

where ω_e and ω_n are angular velocities in the east and north directions, which are calculated from the heading estimation.

Based on the characteristics of pedestrian walking periodicity, a continuity indicator $B_{indicator}$ for pedestrian movement is presented as follows:

$$\begin{aligned} B_{indicator} &= DTW(N, M) \\ N &= (a_{tN1}, a_{tN2}, \ldots, a_{tNn}) \\ M &= (a_{tM1}, a_{tM2}, \ldots, a_{tMm}) \\ a_{ti} &= \sqrt{acc_{x,ti}^2 + acc_{y,ti}^2 + acc_{z,ti}^2} \end{aligned} \quad (7)$$

where N means the acceleration sequence of the previous stride, M means the acceleration sequence of the current stride. DTW is the dynamic time warping algorithm (Jambhale, 2014) that can effectively express the shape similarity of acceleration data of two strides. acc_x, acc_y and acc_z are the measurements around three axes of the acceleration. t is the time variable.

Combining the dynamic indicator $A_{indicator}$ and the continuity indicator $B_{indicator}$, the quality indicator of pedestrian movement is obtained, which is expressed as follows:

$$M_{indicator} = A_{indicator} \cdot B_{indicator} \cdot M_0 \quad (8)$$

where $M_{indicator}$ is the movement quality indicator, M_0 is the empirical factor.

When $M_{indicator}$ is less than a pre-defined threshold, the pedestrian walking quality is considered reliable. The quality indicator of pedestrian movement will be used to adaptively adjust the processing noise of the multi-sensor integration system, thus implementing an adaptive filtering procedure.

2.5 Adaptive Dynamic & Measurement Model

Due to the complexity of indoor environments, the localization performance of smartphone sensors varies in different indoor scenes. Due to the variability of smartphone devices, the measurement error of the built-in sensors on different smartphone varies and is difficult to determine in advance. To tackle this problem, an adaptive integration system based on multi-scene recognition and movement quality monitoring is proposed in this section. It consists of two main components, namely the adaptive estimation measurement noise matrix R and the adaptive adjustment process noise matrix Q.

For the adaptive estimation of the measurement noise matrix R , it is based on a sequence of innovations collected from the previous positioning results. When the indoor scene is identified as a certain scene from multi-scene recognition and the pedestrian walking quality is reliable, the innovation vector of the filtering system is calculated as follows:

$$\alpha_k = z_k - H \cdot x_k^- \tag{9}$$

where α_k is the innovation vector, z_k is the measurement vector, H is the measurement design matrix, x_k^- is the predicted vector after time update, k is the epoch.

The covariance matrix of the innovation vector is calculated as follows:

$$A_{\alpha_k} = R_k + H \cdot P_k^- \cdot H^T \tag{10}$$

where A_{α_k} is the covariance noise matrix of α_k , R_k is the covariance noise matrix of z_k and P_k^- is the covariance noise matrix of x_k^- .

In order to obtain the covariance matrix of the measurements, equation (10) is modified as follows:

$$R_k = A_{\alpha_k} - H \cdot P_k^- \cdot H^T \tag{11}$$

where the innovation covariance matrix A_{α_k} can be computed by averaging inside a estimation window:

$$A_{\alpha_k} = \frac{1}{m} \sum_{i=k-m+1}^{k} \alpha_k \alpha_k^T \tag{12}$$

where m is the window size, α_k is the innovation vector obtained from equation (9). It is worth noting that the R_k value will not be updated when the indoor scene changes or the quality of pedestrian movement is unreliable.

For the adaptive adjustment process noise matrix Q, it relies on the quality monitoring of pedestrian movement. Therefore, the process noise matrix is adaptively adjusted using the quality indicator of pedestrian movement $M_{indicator}$, which is expressed as follows:

$$Q_k = M_{indicator} \cdot Q_0 \tag{13}$$

where Q_0 is the initial system process noise of the multi-sensor integration solution and Q_k is the process noise matrix at the epoch k. The system process noise will increase when the pedestrian movement is unstable or discontinuous. Once the pedestrian movement quality is stable, the integration solution will converge. In turn, the reliability and robustness of the solution is enhanced.

Combining equations (11) and (13), adaptive estimation of the measurement noise matrix and adaptive adjustment of the process noise matrix are obtained. Eventually, an adaptive multi-sensor integration system is achieved.

2.6 Autonomous Outlier Detection

Due to the complexity of the indoor environment, outliers caused by multipath or signal noise are common in real-time positioning. Since different types of localization sensors are incorporated in the integration solution, it is necessary to apply autonomous outlier detection.

Combining equation (10), we obtain the innovation covariance matrix A_{α_k} . And the new innovation vector α_k are calculated by equation (9). When a new innovation measurement is out the confidence interval, it is considered as an outlier, which can be expressed as follows:

$$\alpha_k^{'} > 3 \cdot \sqrt{A_{\alpha_k}^{'}} \tag{14}$$

where $\alpha_k^{'}$ is the new innovation measurement, $A_{\alpha_k}^{'}$ is the innovation covariance value.

The measurement update of the integration system will not proceed and the innovation vector will not be updated until no outliers are detected. This will reliable detect outlier errors online in the integration system. In turn, the stability of the multi-sensor integration system is enhanced.

3. EXPERIMENTS

Several walking tests were conducted in an office building at Wuhan university. It was used for the experiments to test the localization performance of different sensor combinations, as shown in Fig. 2, where the yellow area indicated the QUUPPA coverage area, and the green area indicated the light sensor localization coverage area. This building covered a variety of indoor scenes, such as, corridors, rooms, halls, etc. In both scenarios, the coverage area of the high-precision devices was about 250 m^2, which was about 1/4 of the whole area. Real-time tests were conducted using a Samsung S10 smartphone, whose IMU sensor frequencies were set to 50 Hz. The reference trajectory was based on a LiDAR-based handheld simultaneous localization and mapping (SLAM) device, as shown in Fig. 3, which was capable of centimeter-level positioning accuracy.

We perform the indoor positioning testing in a typical indoor space to verify the positioning accuracy of the proposed solution. The testing area layout and the deployment of high-precision sensors are shown as Fig. 2. This space is fully covered with Wi-Fi signals.

In this scenario, the main scenes include halls, corridors and rooms. The tester walked out of the main hall equipped with light devices with a Samsung S10 smartphone. Then he reached the other areas of Scenario A. Light sensors, Bluetooth AoA system (i.e., QUUPPA system), Wi-Fi and PDR were involved

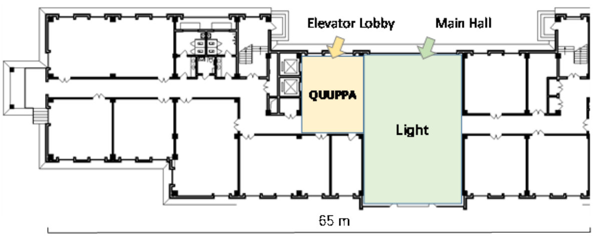

Figure 2. A typical office building equipped with acoustic, light and QUUPPA devices. The low-cost Wi-Fi is fully covered in this scenario.

Figure 3. A handheld SLAM positioning device.

in the real-time multi-sensor integration algorithm throughout the testing process. Plots a, b, c, and d of Fig. 4 depict the light localization results, QUUPPA localization results, Wi-Fi fingerprinting results, and multi-sensor integration localization results, respectively. The corresponding position cumulative error distribution is shown in Fig. 5. As depicted in Figs. 5, the positioning accuracy of the light sensor and QUUPPA is high, reaching 0.33 m (1σ) and 0.75 m (1σ), respectively. However, their positioning coverage area is small, covering only the main hall and elevator lobby areas. The Wi-Fi fingerprinting solution covers all areas of the scenario, but its positioning accuracy is not high, about 3.66 m (1σ). The proposed multi-sensor integration solution combines the advantages of both high and low precision sensors to achieve an accuracy of 0.98 m (1σ) over the entire test area. The maximum positioning errors for these four solutions are 0.67, 2.05, 10.01 and 2.86 m, respectively. The reliability of the proposed solution is improved.

4. CONCLUSIONS

This work proposed an adaptive smartphone hybrid indoor positioning solution incorporating heterogenous sensors to improve the accuracy and wide-area availability of indoor positioning. Combining the knowledge of multi-scene recognition and movement quality monitoring, measurement noise and process noise are adaptive estimated and adjusted in the filtering procedure, and improve the reliability of the integration solution with multiple sensors. The method of autonomous outlier detection is proposed to increase the robustness of the integration solution. By analyzing the positioning characteristics of different positioning sensors, this approach effectively exploits high-precision sensors as controlling anchors and combines low-precision but low-cost

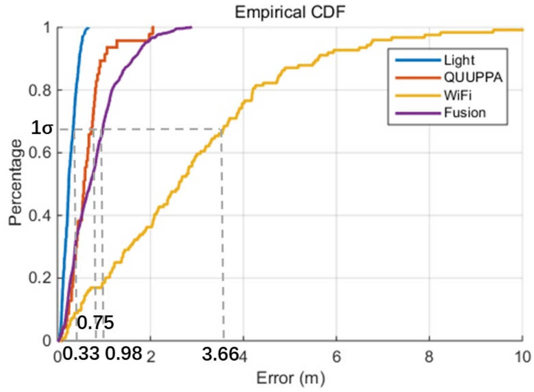

Figure 5. Positioning cumulative error percentages of the four different solutions.

sensors to achieve enhanced positioning accuracy of better than 1 meter and wide-range coverage.
In several experiments, the overall positioning accuracy of the proposed hybrid indoor solution is greatly improved, from 3.66 m to 0.98m. In future work, we will apply the proposed method to other location-based internet of things applications, such as wearable devices, health monitoring and smart hospitals.

REFERENCES

Brovko, T., et al., 2021: Complex Kalman Filter Algorithm For Smartphone-based Indoor UWB/INS Navigation Systems. *USBEREIT*, pp. 0280-0284.

Cao, S. et al., 2020: Effective Audio Signal Arrival Time Detection Algorithm for Realization of Robust Acoustic Indoor Positioning. *IEEE Trans. Instrum. Meas.*, vol. 69, no. 10, pp. 7341-7352

Davidson, P., Piché, R., 2017: A Survey of Selected Indoor Positioning Methods for Smartphones. *IEEE Commun. Surveys Tutorials*, vol. 19, no. 2, pp. 1347-1370.

Harle, R., 2013: A Survey of Indoor Inertial Positioning Systems for Pedestrians. *IEEE Commun. Surveys Tutorials*, vol. 15, no. 3, pp. 1281-1293.

Huggins, K.R., et al., 2009: Computer vision localization based on pseudo-satellites. *Proceedings of the IEEE 2009 National Aerospace & Electronics Conference (NAECON)*, pp. 26-31, doi: 10.1109/NAECON.2009.5426655.

Huo, Y., et al., 2018: Cellular and WiFi Co-design for 5G User Equipment, *2018 IEEE 5G World Forum (5GWF)*, pp. 256-261.

Jambhale, S.S., Khaparde, A., 2014: Gesture recognition using DTW & piecewise DTW. *in Proc. Int. Conf. Electronics & Commun. Systems (ICECS)*, pp. 1-5, doi: 10.1109/ECS.2014.6892646.

Julier, S.J., Uhlmann, J. K., 2004: Unscented filtering and nonlinear estimation. *in Proc. IEEE*, vol. 92, no. 3, pp. 401-422.

Li, Y., et al., 2021: Toward Location-Enabled IoT (LE-IoT): IoT Positioning Techniques, Error Sources, and Error Mitigation. *IEEE Internet Things J.*, vol. 8, no. 6, pp. 4035-4062.

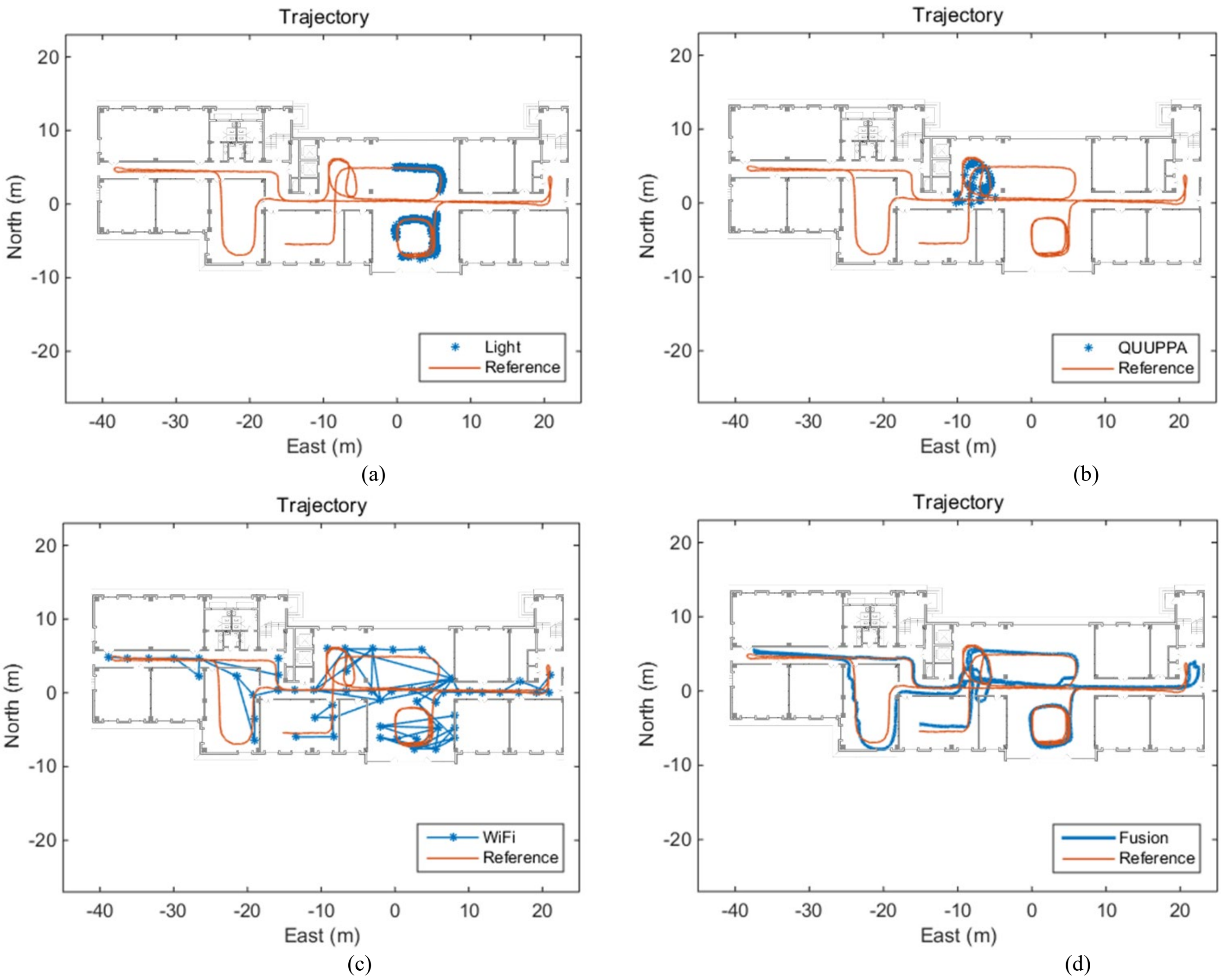

Figure 4. Walking tests of the entire floor in the scenario. (a) Trajectories of the reference and the light solution. (b) Trajectories of the reference and the QUUPPA solution. (c) Trajectories of the reference and the Wi-Fi fingerprinting solution. (d) Trajectories of the reference and the multi-sensor fusion solution.

QUUPPA Company [Online]. Available: http://quuppa.com/company/, Accessed on: Oct. 25, 2021.

Xie, B., et al., 2018: LiPro: light-based indoor positioning with rotating handheld devices. *Wireless Networks*, vol. 24, no. 1, pp. 49-59.

Yang, S., et al., 2021: A Robust Heading Estimation Solution for Smartphone Multisensor-Integrated Indoor Positioning. *IEEE Internet of Things Journal*, vol. 8, no. 23, pp. 17186-17198, doi 10.1109JIOT.2021.3077912.